VNR-AV: Structural Post-processing for Retinal Arteries and Veins Segmentation

Idris Dulau[1,2], Benoit Recur[1,3], Catherine Helmer[1,4], Cecile Delcourt[1,4], and Marie Beurton-Aimar[1,2]

[1] Bordeaux University, France
[2] LaBRI UMR 5800
[3] INSERM LAMC U1029
[4] INSERM U1219
idris.dulau@labri.fr

Abstract. The retinal vasculature reveals numerous health conditions, making the quantitative assessment of changes in retinal arteries and veins crucial for disease prevention and management. Quantifying changes in the retinal vasculature requires segmentation to delineate it. Deep-learning techniques demonstrate impressive results for retinal vasculature segmentation in color fundus images. However, even if the generated segmentations are good at the pixel level, they are not coherent at the structural level, (*i.e.* not anatomically coherent compared to a real retinal vasculature). The vasculature of the retina is composed of two completely connected trees: arteries and veins, whereas segmentations produce several disconnected components. In this article, we propose VNR-AV: a Vasculature Network Retrieval method specifically designed for retinal Arteries and Veins segmentation. The proposed post-processing method achieves two main objectives: it leverages vessels segmentation to enhance the segmentation of arteries and veins by performing reconnection, removal, and detail gathering; and it removes or reconnects segmentation components based on a set of rules developed through an understanding of deep-learning-generated segmentations. VNR-AV retrieve a fully connected thus more anatomically coherent structure of the retinal arteries and veins networks while managing to slightly improve the superposition quality at pixel-level. VNR-AV enable a more coherent assessment of changes in retinal arteries and veins and pave the way for further research in prevention and management of eye-related diseases.

Keywords: Post-processing · Segmentation · Retinal arteries and veins

1 Introduction

The analysis of the fundus, particularly the retinal vasculature, enables the prediction, detection, and monitoring of certain diseases. Specifically, extracting measurements from the retinal network, such as calibers, lengths, and depths, is crucial. To obtain these measurements, it is first necessary to segment the retinal vessels. The generated segmentations should allow for anatomically coherent measurements. VNR-AV, our proposed Vasculature Network Retrieval method specifically designed for retinal Arteries and Veins segmentation, ensures this coherence by retrieving two fully connected trees, one of the arteries and one of the veins. This is achieved through two newly designed sub-processes named *Class Propagation* (see Sec. 3.1) and *Connected Component Retrieval* (see Sec. 3.2). VNR-AV address the challenges of arteries and veins miss-classification along with the reconnection of vascular elements. Miss-classification can occur within a continuous portion of vasculature or along a complete vascular path, while reconnection issues include the presence of artifacts and the absence of vascular paths between components. The results (see Sec. 4) show that VNR-AV successfully retrieves a fully connected structure for both trees, while managing to slightly improve the superposition quality at pixel-level. This enables more coherent measurements of retinal arteries and veins and paves the way for further research in the prevention and management of eye-related diseases.

2 Related Works

Numerous methods from 2019 to 2024, such as [1,2,3,4], propose graph-based solutions to tackle miss-classification issues. This implies that a vascular path, from the optic disc to an endpoint, belongs to a single class. Consequently, these methods propose swapping labels along a path to maintain a single class consistency. However, there are notable problems. First, graph-based methods assume an already connected structure to perform the swaps, which is never the case in such segmentations. Second, these methods operate at graph level, on the skeletonized version of the segmentation, thus measurements on the vasculature such as calibers cannot be accurately retrieved.

Two other methods attempt to tackle miss-classification issues using deep-learning techniques. In [5], a network is trained to restore connectivity given highly disconnected arteries and veins segmentations. In [6], a network is trained to combine three segmentations: binary arteries segmentation, binary veins segmentation, and multi-class arteries and veins segmentation. However, imperfect segmentations generated by deep-learning lead to disconnected elements, failing to produce structurally coherent outputs like a fully connected vasculature.

Some other methods have been developed for vessels segmentation. [7,8] focus exclusively on removing artifacts, whereas [9,10], target reconnections of elements but ignore the presence of artifacts. In [11], both issues are addressed, yet a fully connected structure is not achieved. Conversely, [12] tackles both the presence of artifacts and the absence of vascular paths between components, successfully retrieves a fully connected structure. Despite its effectiveness for vessels segmentation, the latter method cannot be used for arteries and veins segmentation due to significant structural differences in the segmentations.

3 Methods

The proposed VNR-AV method aims to retrieve an anatomically coherent retinal vasculature structure, producing two trees: one of the arteries and one of the veins. This is mainly done by obtaining a structure composed of nearly one connected component (now referred to as CC). VNR-AV operates as a post-processing method on segmentations generated by deep-learning methods, which produce superior pixel-wise results [13]. VNR-AV consists of two distinct sub-procedures: a class propagation, and a CC retrieval. Detailed algorithmic descriptions and Python implementation are accessible at *https://github.com/idrisdulau/*.

3.1 Class Propagation

This is a filling algorithm that leverages vessels segmentations. Constantly, vessels segmentations are more accurately predicted compared to combined arteries and veins segmentations. Given binary segmentations of vessels, arteries, and veins from the same fundus image, it fills the unclassified portions of the vessels segmentations with either the arteries or veins class. The algorithm is composed of three main steps: *SOFT removal* (i), *MERGE* (ii) and *FILL* (iii) (see Fig. 2).

SOFT removal (i) reduces the number of CCs in arteries and veins segmentations. It starts with a binary segmentation of arteries (or veins) and merges it with the corresponding segmentation of the optic disc (OD). This latter is added to reconnect the vasculature, usually poorly connected around this area. The merged result (a) undergoes dilation by a 11*11 kernel and skeletonization (b). These processed outputs (a), (b) are then combined with a *logical or* to connect close CCs in a new image (c) regardless of the connection path. Next, CCs in (c) are removed in increasing area order until five CCs remain. Elements of the skeleton (b) are then deleted from (c) with a *logical and*, resulting in five groups of close CCs but potentially more than five CCs overall. This step removes artifacts that would interfere with (iii), while maintaining a sufficient amount of information that will be further reconnected or removed afterwards. (The 11*11 kernel employed for this dilation is empirically deduced to be the most efficient in preserving information while avoiding artifact gathering.)

MERGE (ii) takes vessels, arteries, and veins segmentations as input. It merges them into an RGB image, further used in the method (iii). In this image, arteries (a) are represented by red pixels and veins (b) by blue pixels. Overlaps (c) are represented by green pixels, and generated by a *logical and* between (a) and (b). Black pixels represent the background. Then, white pixels in vessels segmentation that are black at corresponding position in (a), (b) and (c) are added to the RGB image as white pixels (see Fig. 1, left image).

FILL (iii) assigns white pixels to either the arteries or veins class. It begins by extracting each white CC (a) Then, (b) is obtained by a dilation of (a) with a 3*3 kernel. The contour (c) is obtained by a *subtraction* of (b) by (a). If (c) shows uniform coloration, then (a) is colored accordingly. If (c) displays multiple colors, then (a) is removed, by coloring it black. Fig. 1 illustrates the procedure, with the colorized CCs displayed on the middle, and the final result on the right.

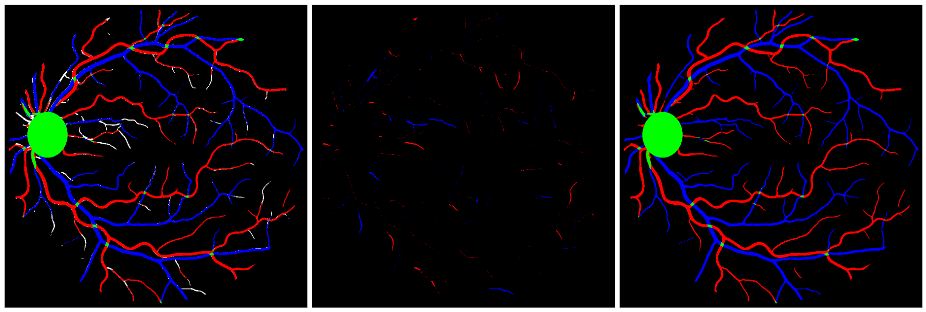

Fig. 1. Example of *MERGE* followed by *FILL* method to fill the unclassified portions of the vessels segmentations with either the arteries or veins class. From left to right: merged input, colorized portions of vessels, filled output

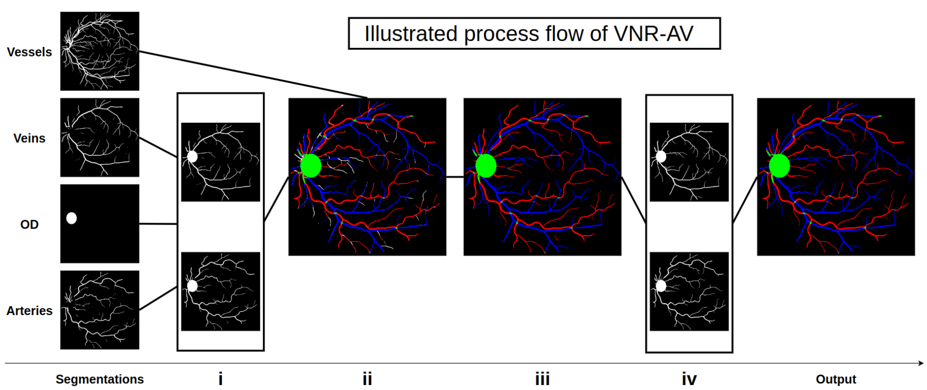

Fig. 2. Illustrated process flow of VNR-AV, composed of four main steps: *SOFT removal* (i), *MERGE* (ii), *FILL* (iii) and *CC retrieval* (iv). VNR-AV takes four binary segmentations as input and produces one RGB segmentation as output

3.2 Connected Components Retrieval

This is an algorithm designed to remove artifacts and reconnect vasculature. Given binary segmentations of arteries and veins, enhanced by steps (i) to (iii), it retrieves two connected trees: one of the arteries and one of the veins (see Fig. 2). The algorithm is composed of several steps summed-up as (iv).

The first component of the method builds upon the approach introduced by [12]; it incorporates the unmodified *Gap Filling* procedure and refines the *Finding candidates* process within the *Rebranch or Remove* procedure. The proposed methodology begins by identifying the main CC (a), which is the largest in terms of pixel area, along with smaller CCs (b). The procedure aims to reconnect each (b) to (a) in decreasing area order or remove them entirely. Each (b) undergoes skeletonization (c), and endpoints (referred to as endP) and crosspoints (referred to as crossP) are extracted from (c). Considering white pixels centered in a 3*3 view: endP are surrounded by exactly one white pixels, and crossP are surrounded by more than two white pixels. For each endP in (c), the nearest crossP within a vascular path (d) is detected. A path going to (a) from (d) through the endP of (c) is computed. The path length in combination with context-specific rules (presented afterwards) will determine the final reconnection path of each (b). The reconnections are performed in the original segmentation (non-skeletonized), using the vascular thickness method of [12].

Additionally, some procedures dictate specific reconnection behaviors based on contextual factors. An example of such specificity is when (b) is smaller but big compared to (a) as illustrated in Fig. 3. This case is caused by an overlap between arteries and veins leading to the miss-detection of one or the other in a certain zone (red rectangles). In such cases, the reconnection path of (b) to (a) must be the closest path between either: an endP of (b) and the OD center, or, an endP of (b) and an endP of (a). As (b) is only reconnected to (a) in the procedure, and to avoid incoherent suppression of many CCs, once (b) is reconnected to (a) the pixels belonging to (a) are updated. This allows reconnection of CCs such as those shown in Fig. 3 (green rectangles).

Fig. 3. Example of a specific reconnection behavior tackled by the CC retrieval procedure. From left to right: the input segmentation, the skeletonized segmentation of the two largest CCs with the generated reconnection path, and the corresponding groundtruth. The red rectangle highlights the reconnection zone, while the green rectangle indicates a CC whose reconnection depends on the previous reconnection.

4 Experiments

4.1 Material

Our proposed VNR-AV is a post-processing method designed to be applied on segmentations generated by deep-learning. Some state-of-the-art methods such as [14], deliver excellent pixel-level segmentation quality, which correlates with good structural connectivity. However, these results are obtained in source-to-source contexts, but segmentations are not that good in real-world applications. To ensure reproducibility and fair performance evaluation, we use segmentations generated by a deep-learning algorithm in few-shot scenarios, as described in [15]. This approach (referred to as VAVnets) reflects real-world conditions and avoids the bias of overly optimized segmentations, providing a robust baseline for assessing the effectiveness of VNR-AV. The available segmentations are generated over four publicly available datasets, where characteristics are sum-up in Tab. 1.

	DRIVE [16]	DUMO [17]	HRF [18]	LESAV [19]
Material	Canon CR5	OT-110M	Canon CR-1	NA
Resolution	565*584	1024*1024	3504*2336	1620*1444
Images	40	30	45	22
Pathologies	7	NA	30	11
Focus	macula	macula	macula	optic disc

Table 1. Characteristics of the datasets used in [15]

4.2 Results & Discussion

VNR-AV is applied to the segmentations generated by VAVnets, with the results shown in Table 2. For each dataset, VNR-AV successfully retrieves a connected structure for both arterial and venous trees. Initially, the segmentations contain an average of 29 to 116 CCs, but after applying VNR-AV, this is reduced to an average of 1.1 to 1.6 CCs. In this way, VNR-AV retrieves a more anatomically coherent structure of the retinal arteries and veins while slightly improving pixel-level superposition quality on average. The dice scores have been computed without considering the OD zone. While the OD position is used for measurement purposes, the vasculature segmentation within this zone is always excluded.

	Arteries								**Veins**							
	DRIVE		DUMO		HRF		LESAV		DRIVE		DUMO		HRF		LESAV	
	dice	CC	dice	CC	dice	CC	dice	CC	dice	CC	dice	CC	dice	CC	dice	CC
VAVnets	0.729	49	0.775	55	0.738	114	0.767	35	0.783	37	0.813	56	0.775	116	0.792	29
VNR-AV	0.733	1.5	0.778	1.5	0.742	1.6	0.773	1.2	0.783	1.4	0.812	1.6	0.780	1.6	0.797	1.1

Table 2. Performances of VNR-AV applied on VAVnets segmentations, for arteries and veins, over four datasets

Good quality samples obtained after the use of VNR-AV are illustrated in Fig. 4. As one can see, both the arteries tree and the veins tree are fully connected. From the VAVnets segmentations, artifacts are removed, disconnected elements are reconnected, and details that are not initially present in the arteries and veins segmentations are retrieved thanks to the use of the vessels segmentations. The final output of VNR-AV is the RGB image, retrieving the overlaps between arteries and veins segmentations.

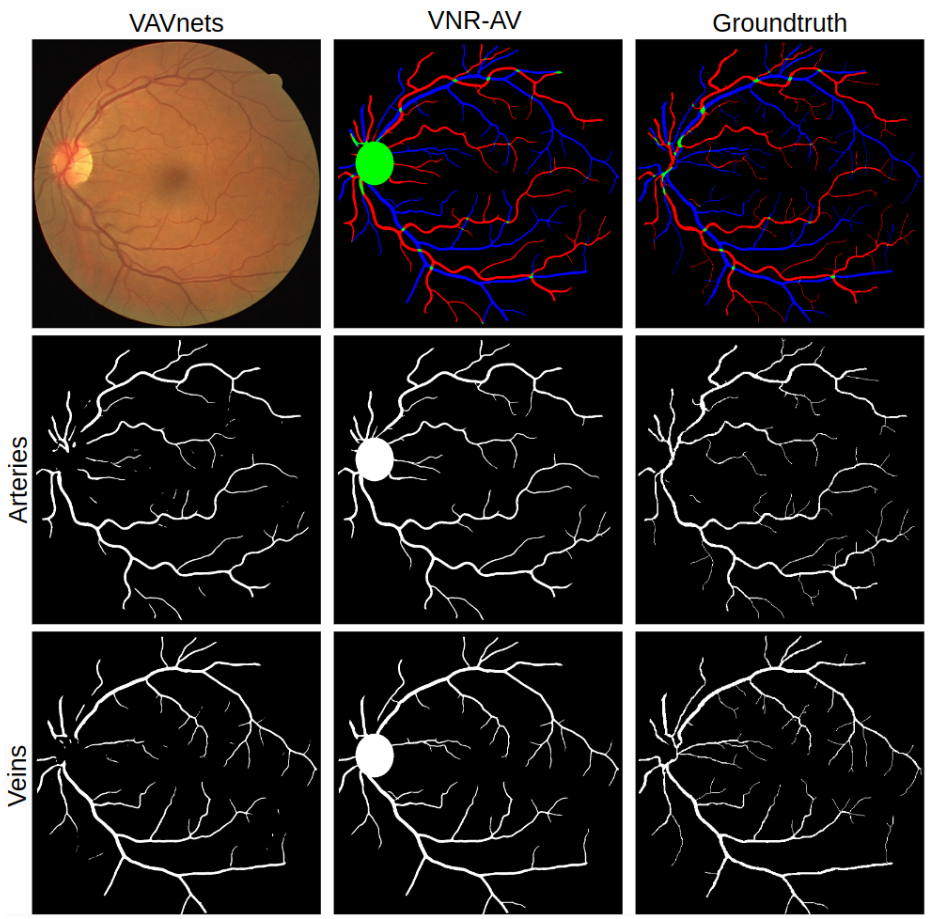

Fig. 4. Example of VNR-AV results compared to the initial segmentation and corresponding groundtruth for arteries and veins

VNR-AV retrieves a fully connected, more anatomically coherent structure of the retinal arteries and veins networks and slightly improves the superposition quality at the pixel level. We first discuss the fully connected aspect and why, instead of obtaining a single CC as expected, we observe an average reduction in segmentation to 1.1 to 1.6 CCs. Although the retinal vasculature is anatomically fully connected, this assumption may not hold within a specific field of view (FOV), resulting in some disconnected CCs within the FOV. We designed the method acknowledging this information, consequently producing segmentations with an average of 1.1 to 1.6 CCs. While VNR-AV addresses most post-processing challenges related to arteries and veins segmentations, some aspects can still be improved. As a human-crafted method, VNR-AV is not perfect; it can delete CCs that are not artifacts and generate incorrect reconnection paths, especially if the initial segmentation quality is poor. Additionally, if the initial segmentations contain significant miss-classifications, achieving a coherent structure becomes impossible. While we consider a post-processing method as VNR-AV crucial for accurate measurements, such post-processing technique have limited potential for further improvement. We believe that achieving an anatomically coherent structure correlated with a high superposition score is the best possible outcome, as the remaining differences in dice scores with the groundtruth are similar as those between groundtruths made by human annotators. Nonetheless, we propose two solutions to ensure better accuracy in future measurements extracted from these segmentations. First, a verification step can be added after applying VNR-AV to check for abnormalities based on human knowledge. For example, detecting a graph pattern within a supposed tree indicates a segmentation error, leading to incorrect measurements. While detecting the graph pattern cannot help refining the segmentation, it can prevent to extract incorrect measurements of the segmentation. Second, a verification step can be added immediately after acquiring the fundus image. Analyzing the image quality at this stage can prompt a re-acquisition if necessary, thereby reducing segmentation errors primarily caused by poor image quality. Improved segmentation leads to better post-processing results which enhances the retrieval of an anatomically coherent structure, thus lead to extract better measurements.

5 Conclusion

We propose VNR-AV: a Vasculature Network Retrieval method specifically designed for retinal Arteries and Veins segmentation. VNR-AV successfully addresses the challenges of arteries and veins miss-classification along with the reconnection of vascular elements. We uniquely offer a class propagation procedure based on vessels segmentation, generate new paths for arteries and veins networks, and ensure a single CC for arteries and veins when necessary, considering the FOV. VNR-AV retrieves a fully connected structure for both arteries and veins trees while slightly improving the superposition quality at pixel- level. This enables more coherent measurements of retinal arteries and veins. Finally, we believe that incorporating verification steps would enhance the overall reliability of the measurements, ensuring that only high-quality segmentations are used for clinical evaluations and research. This would ultimately improve patient care and outcomes in the prevention and management of eye-related diseases.

References

1. F. Girard, C. Kavalec, and F. Cheriet, "Joint segmentation and classification of retinal arteries/veins from fundus images," *Artificial intelligence in medicine*, vol. 94, pp. 96–109, 2019.
2. L. Li, M. Verma, Y. Nakashima, R. Kawasaki, and H. Nagahara, "Joint learning of vessel segmentation and artery/vein classification with post-processing," in *Medical Imaging with Deep Learning*, pp. 440–453, PMLR, 2020.
3. H. Kang, Y. Gao, S. Guo, X. Xu, T. Li, and K. Wang, "Avnet: A retinal artery/vein classification network with category-attention weighted fusion," *Computer Methods and Programs in Biomedicine*, vol. 195, p. 105629, 2020.
4. A. Zhao, H. Su, C. She, H. Li, H. Qiu, X. Huang, and Z. Jiang, "Optimization of retinal artery/vein classification based on vascular topology," *Biomedical Signal Processing and Control*, vol. 88, p. 105539, 2024.
5. W. Chen, S. Yu, J. Wu, K. Ma, C. Bian, C. Chu, L. Shen, and Y. Zheng, "Tr-gan: Topology ranking gan with triplet loss for retinal artery/vein classification," in *Medical Image Computing and Computer Assisted Intervention–MICCAI 2020: 23rd International Conference, Lima, Peru, October 4–8, 2020, Proceedings, Part V 23*, pp. 616–625, Springer, 2020.
6. Y. Zhou, M. Xu, Y. Hu, H. Lin, J. Jacob, P. A. Keane, and D. C. Alexander, "Learning to address intra-segment misclassification in retinal imaging," in *Medical Image Computing and Computer Assisted Intervention–MICCAI 2021: 24th International Conference, Strasbourg, France, September 27–October 1, 2021, Proceedings, Part I 24*, pp. 482–492, Springer, 2021.
7. I. Dulau, B. Recur, C. Helmer, C. Delcourt, and M. Beurton-Aimar, "Connected-components-based post-processing for retinal vessels deep-learning segmentation," in *2023 IEEE 13th International Conference on Pattern Recognition Systems (ICPRS)*, pp. 1–7, 2023.
8. X. Wang, X. Jiang, and J. Ren, "Blood vessel segmentation from fundus image by a cascade classification framework," *Pattern Recognition*, vol. 88, pp. 331–341, 2019.
9. L. Mou, L. Chen, J. Cheng, Z. Gu, Y. Zhao, and J. Liu, "Dense dilated network with probability regularized walk for vessel detection," *IEEE transactions on medical imaging*, vol. 39, no. 5, pp. 1392–1403, 2019.
10. V. S. Joshi, M. K. Garvin, J. M. Reinhardt, and M. D. Abramoff, "Identification and reconnection of interrupted vessels in retinal vessel segmentation," in *2011 IEEE International Symposium on Biomedical Imaging: From Nano to Macro*, pp. 1416–1420, IEEE, 2011.
11. H. Du, X. Zhang, G. Song, F. Bao, Y. Zhang, W. Wu, and P. Liu, "Retinal blood vessel segmentation by using the ms-lsdnet network and geometric skeleton reconnection method," *Computers in Biology and Medicine*, vol. 153, p. 106416, 2023.
12. I. Dulau, C. Helmer, C. Delcourt, and M. Beurton-Aimar, "Ensuring a connected structure for retinal vessels deep-learning segmentation," in *Proceedings of the IEEE/CVF International Conference on Computer Vision (ICCV) Workshops*, pp. 2364–2373, October 2023.
13. A. Khandouzi, A. Ariafar, Z. Mashayekhpour, M. Pazira, and Y. Baleghi, "Retinal vessel segmentation, a review of classic and deep methods," *Annals of Biomedical Engineering*, vol. 50, no. 10, pp. 1292–1314, 2022.
14. J. Fhima, J. Van Eijgen, H. Kulenovic, V. Debeuf, M. Vangilbergen, M.-I. Billen, H. Brackenier, M. Freiman, I. Stalmans, and J. A. Behar, "Lunet: Deep learning

for the segmentation of arterioles and venules in high resolution fundus images," *arXiv preprint arXiv:2309.05780*, 2023.

15. "Vavnets: retinal vasculature segmentation in few-shot scenarios," *Progress in Pattern Recognition, Image Analysis, Computer Vision, and Applications, under review*, 2024.
16. J. Staal, M. D. Abràmoff, M. Niemeijer, M. A. Viergever, and B. van Ginneken, "Ridge-based vessel segmentation in color images of the retina," *IEEE Transactions on Medical Imaging*, vol. 23, pp. 501–509, 2004.
17. S. Zhang, R. Zheng, Y. Luo, X. Wang, J. Mao, C. J. Roberts, and M. Sun, "Simultaneous arteriole and venule segmentation of dual-modal fundus images using a multi-task cascade network," *IEEE Access*, vol. 7, pp. 57561–57573, 2019.
18. J. Odstrcilík, R. Kolář, A. Budai, J. Hornegger, J. Jan, J. Gazárek, T. Kubena, P. Cernosek, O. Svoboda, and E. Angelopoulou, "Retinal vessel segmentation by improved matched filtering: evaluation on a new high-resolution fundus image database," *IET Image Process.*, vol. 7, pp. 373–383, 2013.
19. J. I. Orlando, J. B. Breda, K. van Keer, M. B. Blaschko, P. J. Blanco, and C. A. Bulant, "Towards a glaucoma risk index based on simulated hemodynamics from fundus images," in *International Conference on Medical Image Computing and Computer-Assisted Intervention*, 2018.